Supporting Information

"Visualization and Characterization of Metallo-Aggregates using Multi-photon Microscopy"

Ana Zamora,[a] Michèle Moris,[a] Rui Silva,[a,b] Olivier Deschaume,[b] Carmen Bartic,[b] Tatjana Parac-Vogt[c] and Thierry Verbiest.[a]

[a]*Molecular Imaging and Photonics, KU Leuven, Belgium,* Email: anamaria.zamoramartinez@kuleuven.be.

[b]*Engineering Faculty of Oporto University, Portugal (FEUP) and Abel Salazar's Biomedical Sciences Institute, Portugal (ICBAS)*

[c]*Laboratory for Soft Matter and Biophysics, KU Leuven, Belgium.*

[d]*Laboratory of Bioinorganic Chemistry, Department of Chemistry, KU Leuven, Belgium.*

Table of Contents

1. General Methods and Materials:

All synthetic manipulations were performed under inert atmosphere by using standard Schlenk techniques. All chemicals were obtained from common commercial sources and used without further purification. *N,N'*-didecyl-2,2'-bipyridine-4,4'-dicarboxamide[1] and the cyclometalated Ir(III) dimer,[2] $[(C^N)_2Ir(N^N)]_2$, were synthesized as published elsewhere. ^1H and ^{13}C NMR spectra were recorded with a Bruker Avance 600 spectrometer (Bruker, Karlsruhe, Germany), operating at 600 for ^1H and 150 MHz for ^{13}C. Chemical shifts are cited relative to $SiMe_4$ (^1H and ^{13}C, external). Mass analyses were performed with a Thermo Finnigan LCQ Advantage mass spectrometer. UV/Vis absorption spectra were recorded on a Jasco V-730 spectrometer. OPE spectra were recorded on an Edinburgh Instruments FS920 steady state spectrofluorimeter. MPE spectra were recorded on a home-made nonlinear optical scattering setup[3] consisting of a SpectraPhysics Insight DeepSee femtosecond pulsed laser ($\lambda_{exc,\ MPE}$ = 900 nm, 50mW), a Bruker SureSpectrum 500 is spectrometer and an Andor iXon 897 EMCCD camera. There was a 90° angle between the excitation and collection path. A SCOTT KG5 filter was used to eliminate laser light in the collection path. For multi-photon microscopy an Olympus BX61 WI-FV1200-M microscope with a SpectraPhysics Insight DeepSee femtosecond pulsed laser as a high-power light source ($\lambda_{exc,\ MPE}$ = 900 nm, 50 mW) was used. The two-photon emission cross-section of complex **1** in MeOH was calculated at 900 nm of laser irradiation using Rhodamine B as a reference.[4] A Nikon 60xW (NA 1.0) water immersion objective was used for magnification and the fluorescent images were detected in reflection by a Hamamatsu R3896 photomultiplier tube. A stacked image

was constructed by scanning the sample over a range of ~12 µm in the z-plane with steps of 0.65 µm and combining these images. An Agilent 5500 AFM system with MSNL-F cantilevers (f = 110−120 kHz, k = 0.6 N/m, average tip radius of 2−12 nm) was used for topographical imaging in intermittent contact (AAC) mode. The AFM topography images were leveled, line-corrected and measured (height profiles) using Gwyddion. For AFM analysis, the vesicles were deposited on a silicon (anionic) substrate freshly cleaned with piranha solution.
The cross section area of the vesicles was calculated based on a rectangle model with half a circle at both sides so that A= (depth/2)²*PI+(width-depth)*depth).

2. Synthesis and Characterization:

Complex 1. The cyclometalated iridium(III) chloro-bridged dimer (150 mg, 0.123 mmol) and *N,N'*-didecyl-2,2'-bipyridine-4,4'-dicarboxamide (135 mg, 0.259 mmol) were dissolved in dichloromethane/methanol (2:3, v/v) in a round-bottomed flask. The mixture was stirred at 60 ºC for 24 h under argon atmosphere. After cooling the solution to room temperature, an excess amount of KPF_6 (2.5 mmol) was added and the mixture was stirred for 30 min. The crude product was purified by column chromatography using DCM:MeOH:AcOH (94:5:1) as eluent. The solvent was removed under reduced pressure and the product extracted with NaOH 0.1M (10 mL), Milli-Q H_2O (10 mL) and brine (10 mL). The solvent was reduced and the product precipitated as a yellow solid by adding a few drops of a saturated aqueous solution of KPF_6. The product was then filtrated, washed with water and dried under vacuum. Yellow solid. Yield: 59 %

^{1}H NMR (600 MHz, CD_3CN): δ (ppm) = 9.01 (s, 1H), 8.35 (d, J=8.6 Hz, 2H), 8.15 (d, J=5.7 Hz, 2H), 7.94 (t, J=8.1 Hz, 2H), 7.85 (dd, J=5.8, 1.02 Hz, 2H), 7.62 (d, J=5.7 Hz, 4H), 7.10 (t, J=6.9 Hz, 2H), 6.75 (td, t, J=11.9, 1.9 Hz, 2H), 5.75 (dd, J=8.6, 2.1 Hz, 2H), 5.47 (s, 1H), 3.42 (q, t, J=6.6 Hz, 2H), 1.63 (quint, J=6.8 Hz), 1.29 (brs, 28H), 0.89 (d, J=8.4 Hz, 2H); ^{13}C NMR (150 MHz, CD_3CN): δ (ppm) = 163.79, 157.06, 152.87, 150.76, 146.00, 140.77, 127.42, 125.06, 124.82, 123.91, 100.03, 41.03, 32.69, 30.11, 30.06, 29.99, 27.71, 23.45, 14.45; MS (ESI^+, ACN): m/z 1095.4 $[M–PF6]^+$.

Compound **1** was converted to Cl^- salt by dissolving 7 mg of product in 1–2 mL methanol. The dissolved product was loaded onto an Amberlite IRA-410 chloride ion exchange column, eluted with methanol, and the solvent was removed in vacuo.

Nsno-aggregates, NA1. 1,2-Dipalmitoyl-sn-glycero-3-phosphocholine (DPPC, 0.9 mg, 3 eq.) and the amphiphilic Ir(III) complex (0.5 mg, 0.403 µmol, 1 equiv.) were dissolved in a 1:1 $CHCl_3$:MeOH solution (2 mL). After evaporation of the solvents from the product placed in a flask fitted with septum and needle in a vacuum oven at 50 °C, a thin film was obtained which was rehydrated with hot water (2 mL, 70 °C). To improve the solubility, the suspension was treated in a 180 W sonicator with a thermostatic bath at 65 °C for 30 min. CTAB (1.5 mg, 10 eq.) was added as a surfactant followed by another 30 min of sonication to fulfill the process of nano-aggregate formation. Water was evaporated in a flask with septum and needle fitted in a vacuum oven overnight at 50 °C leaving a thin film. The thin film was rehydrated with Milli-Q water (2 mL) and sonicated for 30 min.
The aggregates containing the chloride salt of the photosensitizer, **1** (Cl), were

prepared similarly as well as the nano-aggregates **NA1** without the surfactant, in which the addition of CTAB in last step was skipped.
Vesicles composed of **1**(PF_6): DPPC: NaDPPE-PEG2K were prepared in a 1: 10: 0.1 molar ratio following a previously reported protocol.[5]

3. Additional Figures:

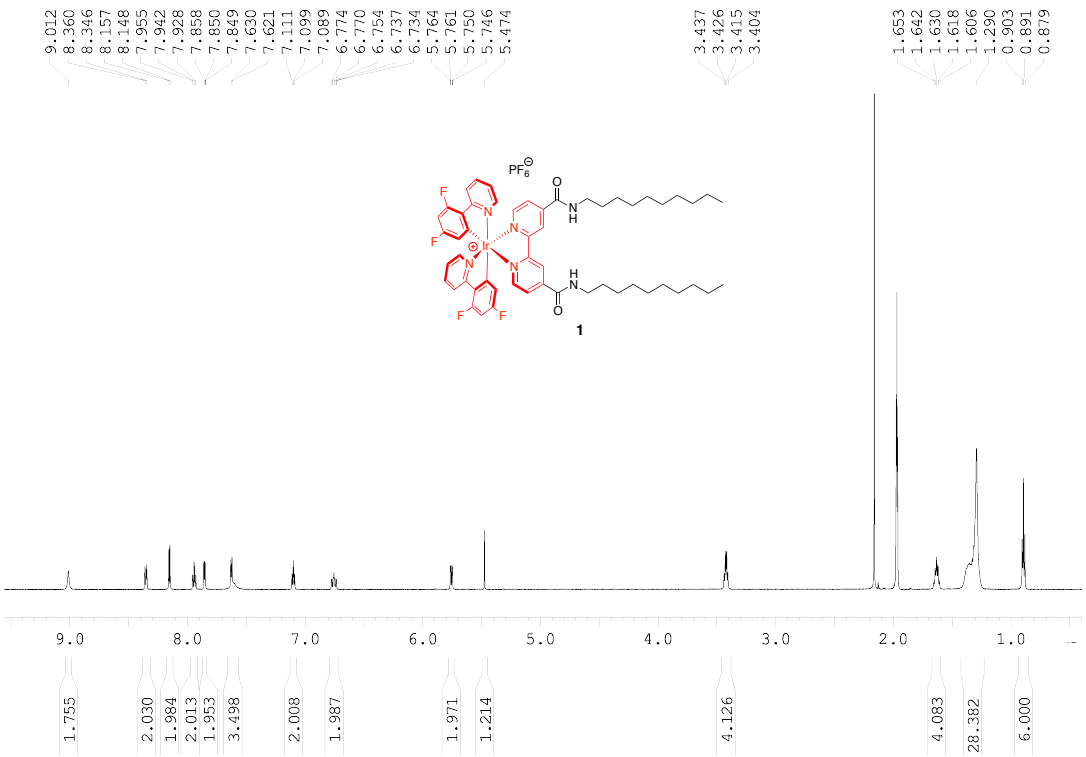

Figure S1. ^{1}H NMR spectrum of **1** (600 MHz, CD_3CN).

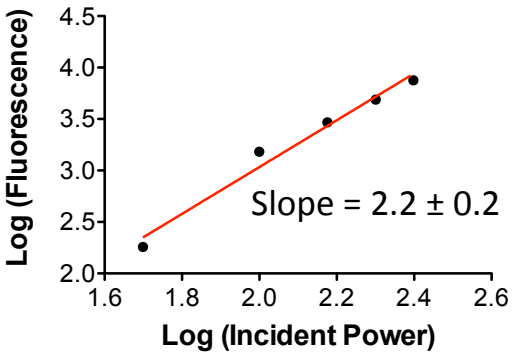

Figure S2. Log-log plot of the fluorescence emission of **1** versus the incident laser power.

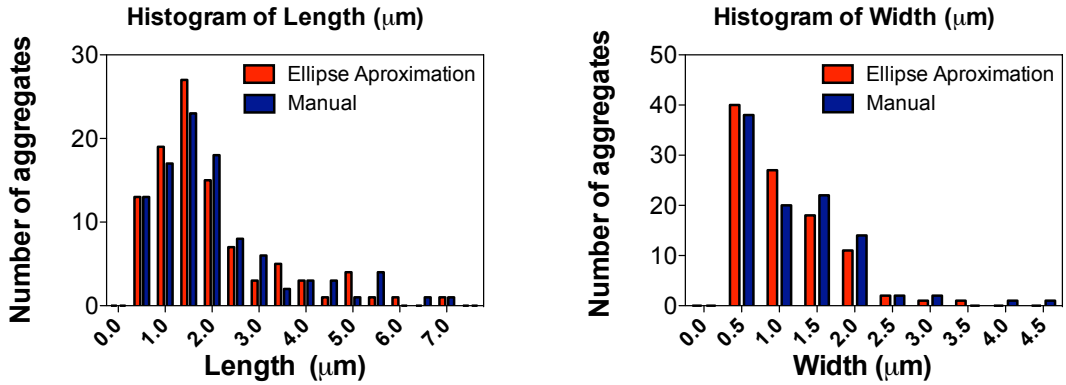

Figure S3. Histograms of length (left) and width (right) of **NA1** when measured manually or using the ellipse approximation.

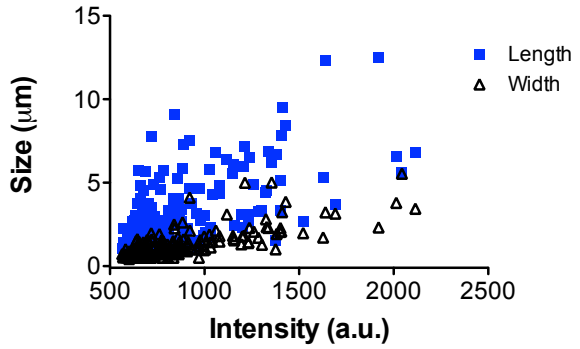

Figure S4. Correlation between the emission intensity of the structure and their length and width.

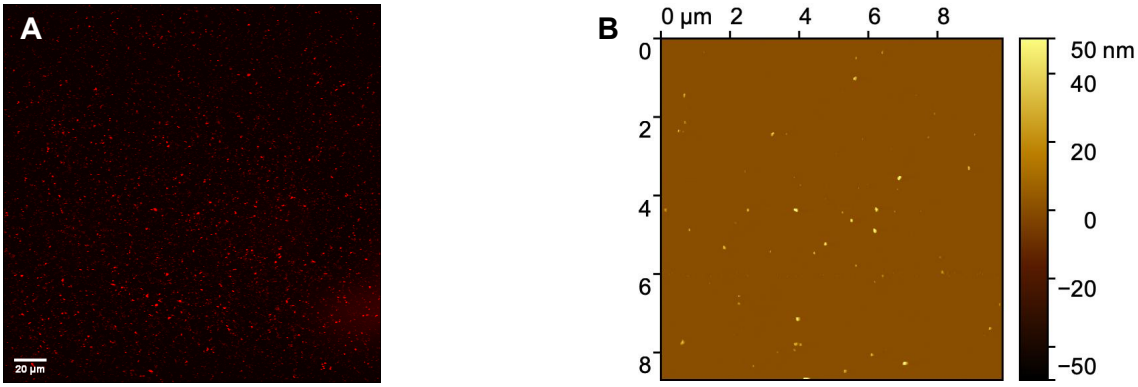

Figure S5. Multi-photon microscopy (A) and AFM (B) images of aggregates containing **1** (Cl) in H_2O.

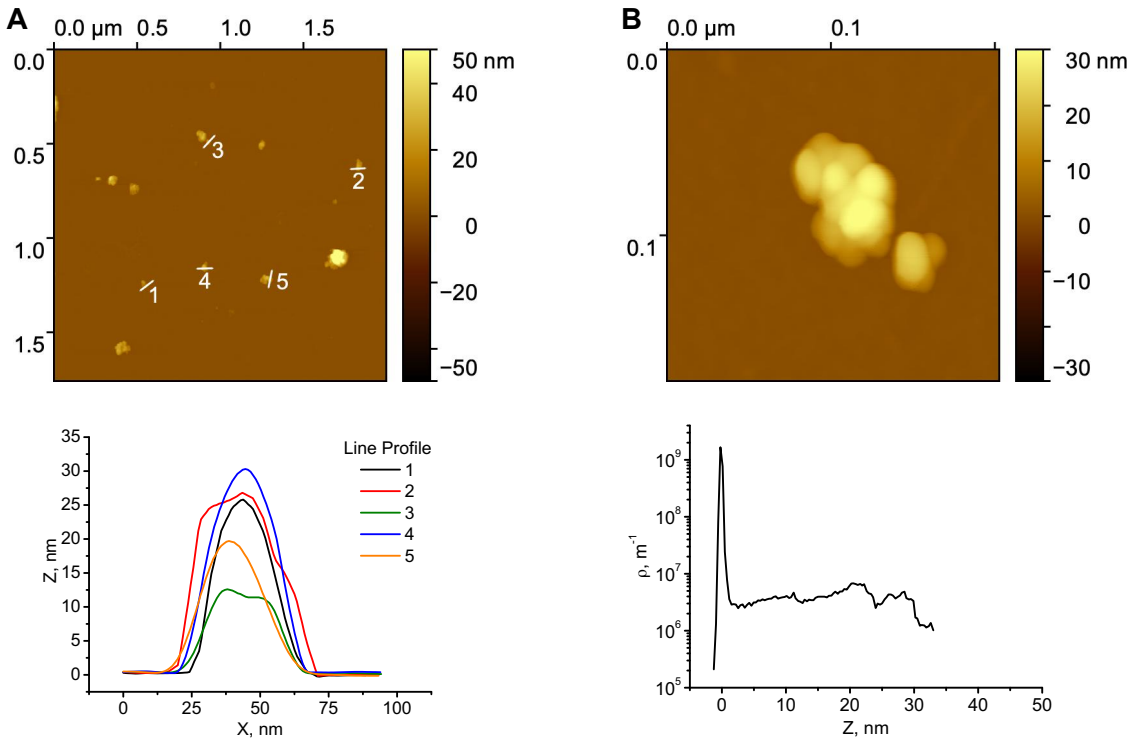

Figure S6. AFM images of aggregates containing **1** (Cl) in H_2O. (A) Display of several large and smaller aggregates; (B) Higher resolution image of one aggregate. The line profiles (C) are taken from the image of panel A and the height distribution (D) from the close-up image of panel B. AFM demonstrates that the aggregates present a curved surface, with no apparent step, and only a few broad peaks are visible in the height distribution.

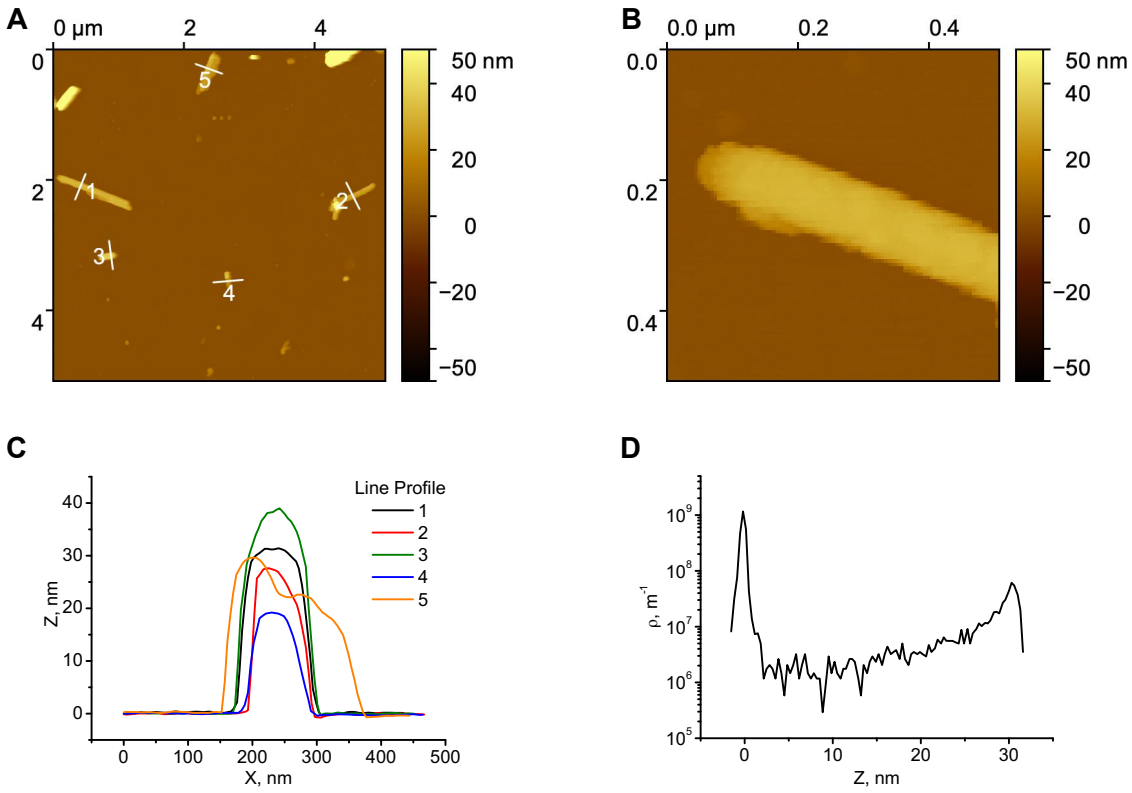

Figure S7. AFM images of the rod-like Ir(III) nano-aggregates **NA1**. (A) Large scan range showing several nano-aggregates displaying a range of diameters and lengths. (B) Close-up image showing the end of one of the rod-like nano-aggregates. The line profiles (C) are taken from the image of panel A, and the height distribution (D) from the close-up image of panel B. AFM line profiles show a curved topography similar to that obtained for the spherical aggregates, albeit with a higher width to height aspect ratio which may arise in part from the rectangular section of the aggregate morphology discussed in the main text. The height distribution presents one peak at ~ 30 nm, in addition to that assigned to the background surface (at 0 nm), with a sharper shape than that observed for spherical aggregates, due to the equal height of the nano-aggregate along its longitudinal axis.

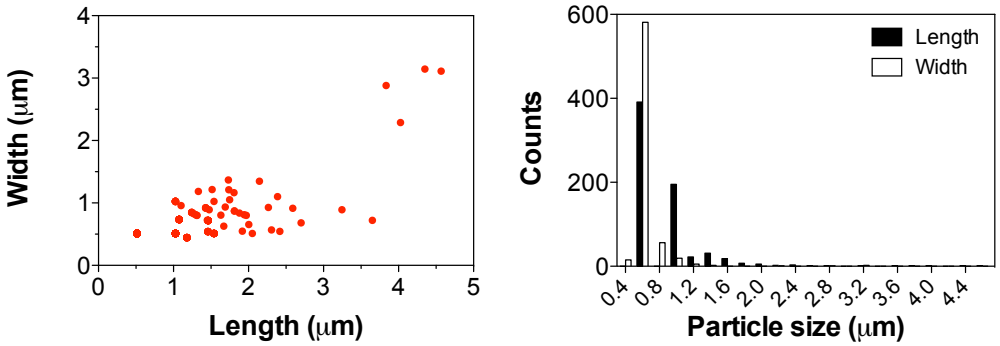

Figure S8. Calculated length and width of aggregates of **1** in MeOH:H_2O (80:20, v/v) (left) and their size distribution (right).

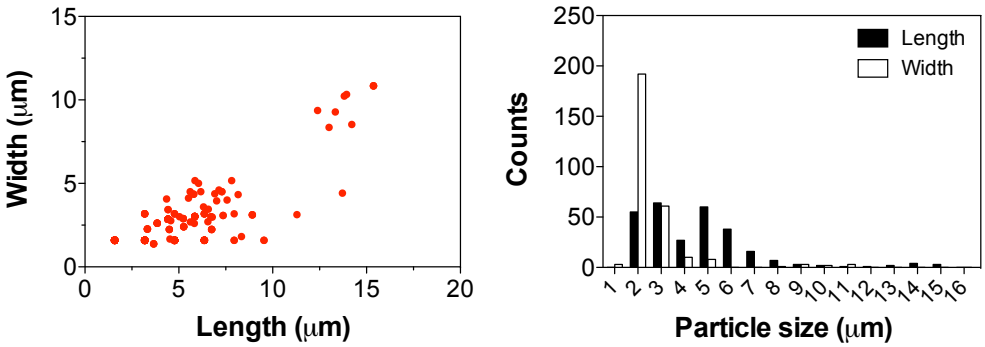

Figure S9. Calculated length and width of aggregates of **1** in H_2O (left) and their size distribution (right).

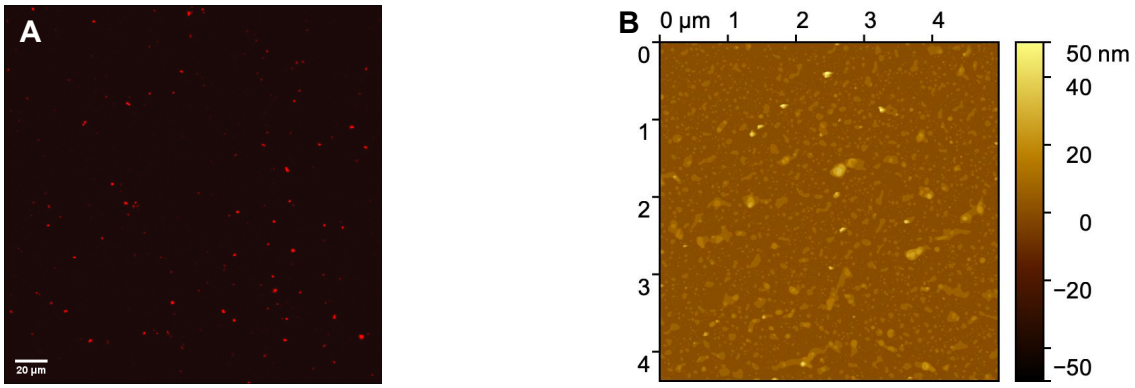

Figure S10. Multi-photon microscopy (A) and AFM (B) images of aggregates containing **1** (PF_6): DPPC in H_2O. No CTAB was added.

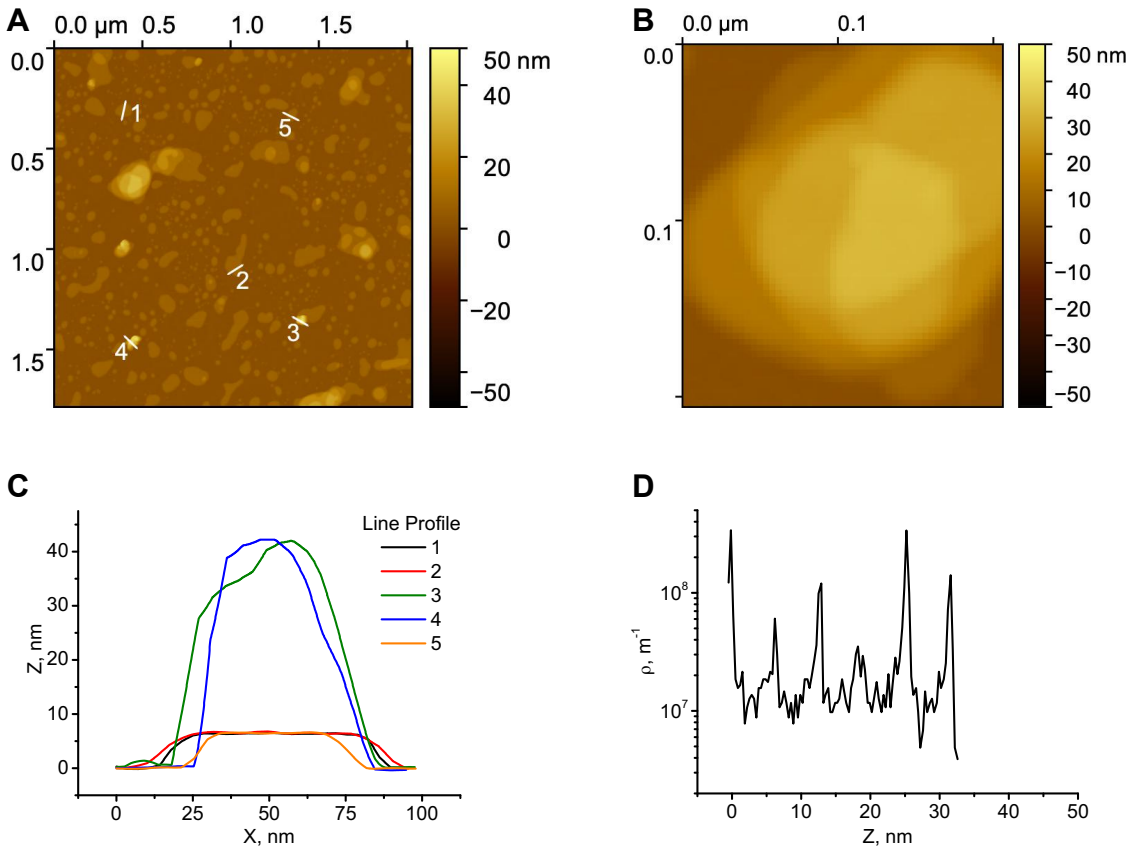

Figure S11. AFM images of structures obtained in the absence of CTAB. (A) Large scan range showing mostly lipid multilayers with their characteristic flattened topography, together with a few, taller aggregates. (B) Higher resolution image showing a multilayer structure, with a characteristic step-like topography. The line profiles (C) are taken from the image of panel A, and height distribution (D) from the close-up image of panel B. AFM line profiles clearly show the distinction between the curved topography of two aggregates, and the flat topography with identical heights for three lipid multilayers, representative for most of the structures present for this sample. The height distribution presents equally spaced, sharp height peaks, characteristic of overlayed lipid multilayers.

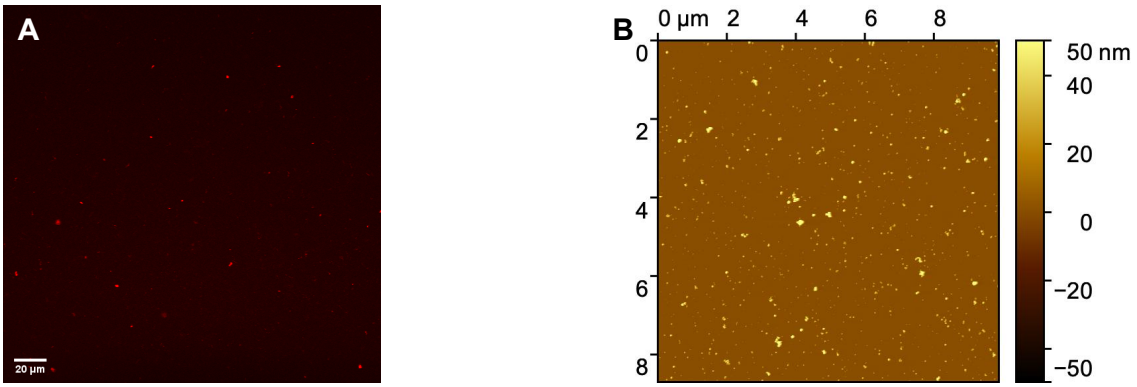

Figure S12. Multi-photon microscopy (A) and AFM (B) images of vesicles containing **1** (PF_6): DPPC: NaDPPC-PEG2K in HEPES buffer (10 mM, *I* = 50 mM, pH 7.4). Images were taken after ulterior dilution to 50 µM of the photosensitizer **1** (PF_6).

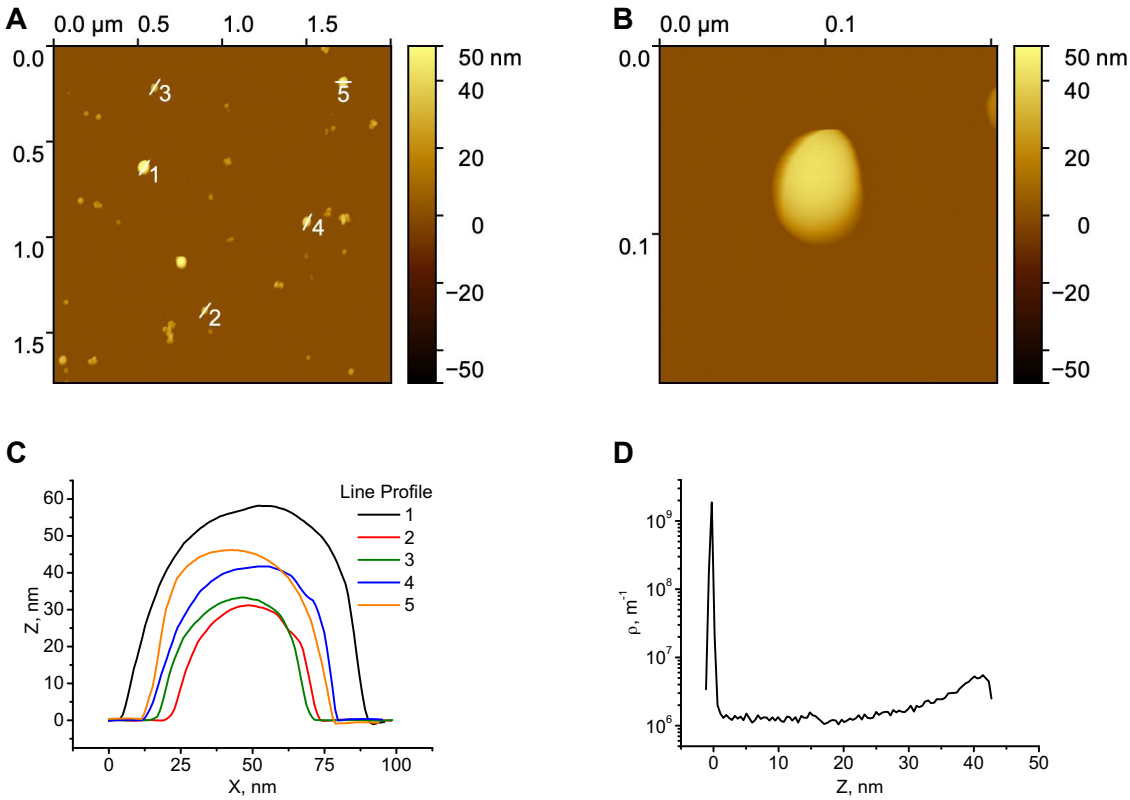

Figure S13. AFM images of vesicles containing **1** (PF_6): DPPC: NaDPPC-PEG2K in HEPES buffer (10 mM, I = 50 mM, pH 7.4). (A) Display of several large and smaller vesicles; (B) Higher resolution image of one liposome. The line profiles are taken from the image of panel A, and the height distribution from the close-up image of panel B. AFM confirms that the vesicles present a curved surface, with no apparent steps, and only a few broad peaks are visible in the height distribution.

4. References

1. C. Sahin, A. Goren, S. Demir, M. S. Cavus, *New J. Chem.,* 2018, 42, 2979-2988.
2. J. Pracharova, G. Vigueras, V. Novohradsky, N. Cutillas, C. Janiak, H. Kostrhunova, J. Kasparkova, J. Ruiz, *Chem. Eur. J.,* 2018, 24, 4607-4619.
3. N. Van Steerteghem, K. Clays, T. Verbiest, S. Van Cleuvenbergen, *Anal. Chem.* **2017**, 89, 5, 2964- 2971.
4. N. S. Makarov, M. Drobizhev, A. Rebane, *Opt. Express* **2008**, 16, 4029-4047.
5. B. Limburg, J. Wermink, S. S. van Nielen, R. Kortlever, M. T. M. Koper, E. Bouwman, S. Bonnet, *ACS Catal.* **2016**, 6, 5968−5977.